Motion-corrected reconstruction of parametric images from dynamic PET data with the Synergistic Image Reconstruction Framework (SIRF)

Richard Brown, *Member, IEEE*, Benjamin A. Thomas, Alaleh Rashidnasab, Kjell Erlandsson, Evgueni Ovtchinnikov, Edoardo Pasca, Andrew Reader, Julian C. Matthews, *Member, IEEE*, Charalampos Tsoumpas, *Senior Member, IEEE*, and Kris Thielemans, *Senior Member, IEEE*

***Abstract*—Motion correction has been added to a PET-MR reconstruction tool, SIRF, by incorporating a registration package, NiftyReg. New functionality has been demonstrated in the context of estimating kinetic parameters in the left temporal lobe, comparing direct and indirect reconstructions and evaluating the impact of using motion correction.**

Principal component analysis was used to detect motion and to determine time frames, while STIR's parametric-OSEM was used to perform the motion-corrected direct parametric reconstruction.

It was found that the variance in the left temporal lobe decreased when motion correction was performed, and the same was true of direct reconstructions compared to indirect.

With SIRF, the entirety of the demonstrated functionality can be performed from a single Matlab or Python script.

I. Introduction

HYBRID PET-MR is an increasingly useful tool. The PET component allows for the extraction of functional information from dynamic PET data using kinetic models. Moreover, the accuracy of these extracted properties could potentially be improved with the use of MR-derived information.

Motion of the patient during scans (respiratory, cardiac or general motion) can cause image blurring, resulting in potentially misleading results. For this reason, motion correction (MC) is currently being incorporated into the Synergistic Image Reconstruction Framework (SIRF) [1], which is available at www.ccppetmr.ac.uk.

SIRF is an open-source framework, aimed at providing researchers with a powerful and flexible platform on which to perform their PET-MR reconstructions. Furthermore, users are also able to easily prototype and implement new reconstruction techniques.

This research is a continuation of previous work [2], extending MC in SIRF from static frame-by-frame reconstruction to direct parametric reconstruction. To demonstrate this new functionality, MC direct parametric analysis (MC direct) is compared to MC indirect analysis (MC indirect) and direct analysis without MC (noMC direct).

Although the example given in this work is PET-MR, the current work is equally applicable to dynamic PET-CT.

Richard Brown, Benjamin A. Thomas, Alaleh Rashidnasab, Kjell Erlandsson and Kris Thielemans are with University College London, Institute of Nuclear Medicine, London, United Kingdom. Evgueni Ovtchinnikov and Edoardo Pasca are with UKRI STFC, Oxfordshire, United Kingdom. Andrew Reader is with Kings College London, Biomedical Engineering Department, London, United Kingdom. Julian C. Matthews is with University of Manchester, Division of Neuroscience and Experimental Psychology, Manchester, United Kingdom. Charalampos Tsoumpas is with University of Leeds, Leeds Institute of Cardiovascular and Metabolic Medicine, Leeds, United Kingdom.

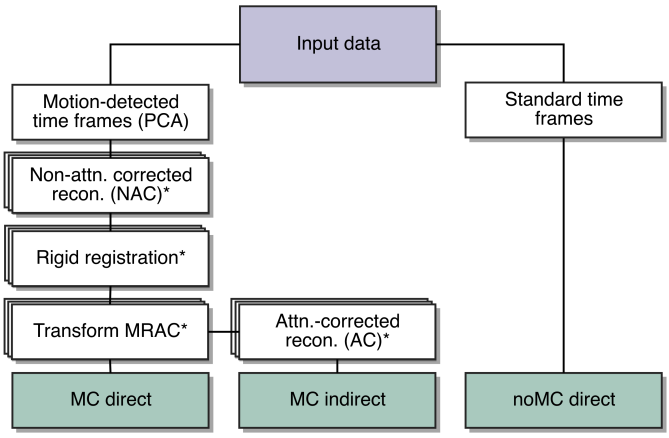

Fig. 1: Workflow for MC direct, as well as MC indirect and noMC indirect. Boxes denoted with * are done on a frame-by-frame basis.

II. Materials and Methods

The example used throughout this work is that of an FDG brain scan, which was taken as part of an epilepsy study. Dynamic PET and MR data were acquired on a Siemens Biograph mMR. PET listmode data and associated normalisation files, MRAC and an MPRAGE image were used for further off-line processing. The corresponding MR-based parcellation was generated with FreeSurfer [3].

A. Reconstruction workflow using motion correction

A simplified workflow for producing the three methods to be compared (MC direct, MC indirect and noMC direct) can be seen in Fig. 1.

Principal component analysis (PCA) was used to determine when motion occurred during the scan, and the listmode data were split into sinograms accordingly [4], [5]. Non-attenuation corrected (NAC) frame-by-frame reconstruction was then performed, such that the frames could be registered (see the following section for more information) to a reference frame. The MR data (the MRAC, MPRAGE and the parcellation) were also registered to the reference frame.

Direct parametric reconstruction was then performed by supplying the motion information (in the form of a displacement field image) and deformed MRAC for each frame. Since the study in question used FDG, Patlak analysis was performed to estimate K_i values. The direct reconstruction algorithm is described in [6], [7]. The SIRF implementation is a wrapper around the well-established STIR library for PET reconstruction [8].

The MC indirect analysis was performed using frame-by-frame attenuation-corrected (AC) reconstruction, where the resulting AC images were resampled into the reference space. The noMC direct analysis was performed by using frames of standard duration (i.e., PCA was not used to detect motion), and no motion information was given to the parametric reconstruction algorithm.

B. Registration

The concept of SIRF is to provide the user with the choice of reconstruction packages, which can be used interchangeably. This idea has been extended to the registration framework, SIRFReg [2]; the user should be able to call different registration packages from a common interface that is easily executable via C++, Python or Matlab.

NiftyReg [9] is the first registration package that has been incorporated into SIRF, providing both affine and rigid ($aladin$) and non-rigid ($f3d$) registrations. NiftyReg's resampling functions have also been exposed in SIRF.

Although the example of rigid registration is given in this work (since the application is head motion), non-rigid registration is equally supported. The simplicity of SIRF's Python/Matlab wrapper code for registration is demonstrated below.

```
reg = mSIRFReg.NiftyAladin();
reg.set_reference_image_filename(ref_file);
reg.set_floating_image_filename(flo_file);
reg.set_parameter_file(param_file);
reg.update();
reg.save_transformation_matrix(TM_file);
reg.save_inverse_transformation_matrix(ITM_file);
reg.save_warped_image(warped);
```

Code 1: Registration with SIRF in Python/Matlab.

C. Reconstruction

NAC, AC and parametric reconstructions were all performed throughout this study. These were done in SIRF with STIR's OSEM and Parametric-OSEM (POSEM) algorithms [8].

The POSEM algorithm has been enhanced such that displacement field images (easily produced from the transformation matrices) for each frame can also be supplied. If present, the image will be transformed before forward projection and after backprojection. The backprojection uses the transpose operation of the forward deformation.

The OSEM and POSEM reconstructions were performed with 7 subsets over a total of 70 image updates.

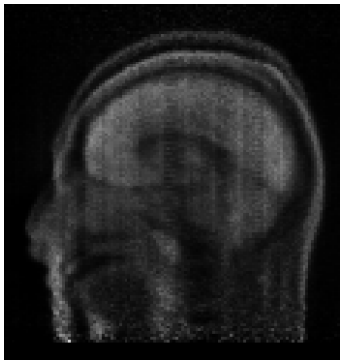

Fig. 2: NAC reconstruction over the duration of the whole scan, to give an idea of motion that occurred.

The output of the indirect parametric reconstruction with MC was smoothed and then used as the initial estimate for the direct parametric reconstruction.

D. Patlak analysis

The input function was determined by fitting a population-based input function to the data. This was done by segmenting the carotids on the MPRAGE and superposing the resulting mask on each decay-corrected, AC frame. Partial volume correction was then performed using the single-target correction model (only correcting the carotids) implemented in [10]. Patlak plots were then generated by superposing the MR-derived parcellation of the chosen volume of interest (VOI), the left temporal lobe. The MC Patlak plot was used to determine when equilibrium had been reached and therefore Patlak analysis could begin.

III. Results and Discussion

Fig. 2 shows an NAC reconstruction over the duration of the whole scan (from 0 to 2700 s). This gives an idea as to the amount of motion that occurred during the scan and shows that, without MC, the reconstructed parametric image might be susceptible to quality degradation.

Fig. 3 shows the first three principal components plotted for the last 2000 s of the scan (the portion of the scan that is interesting for Patlak analysis). Rapid fluctuations in the PCA signals were interpreted as patient motion (since such changes could not be due to the radiotracer redistribution).

It can be seen that three sections of the scan were discounted due to patient movement. The time frames for the parametric analysis were based on standard time frames, and modified to account for motion.

Shown in Fig. 4 is the Patlak plot for the chosen VOI, the left temporal lobe. From the Patlak plots with MC, it was determined that the VOI was in equilibrium from around 750 s (R^2 of 0.984), so the analysis was carried out from this time point until the end of the acquisition (2700 s), comprising a total of 7 frames. From Fig. 4, it can be seen that a noticeable perturbation occurs at 900s in the transformed Patlak curve. This corresponds to the time when rapid changes were observed in the PCA signals, which were interpreted as a period of rapid patient motion.

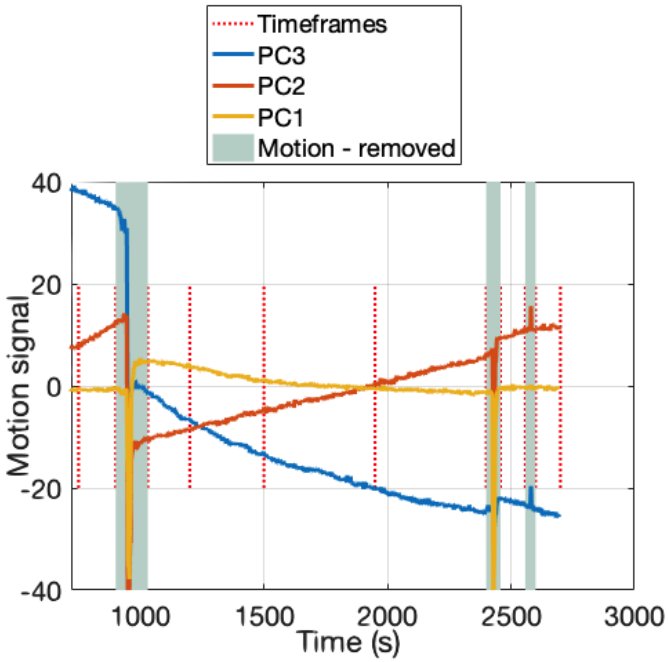

Fig. 3: PCA plot over the last 2000 s of the scan. Large changes in the motion signal indicate patient motion. The resulting time frames are also shown.

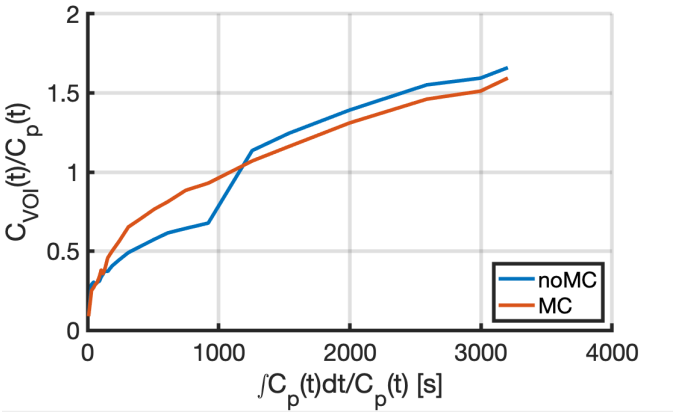

Fig. 4: Patlak plots of the left temporal lobe, both with and without motion correction.

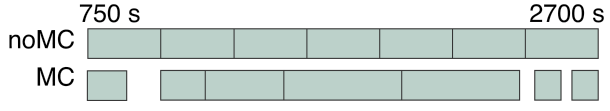

Fig. 5: Time frames for noMC and MC (direct and direct) of the section of the scan to be used for Patlak analysis (750 - 2700 s).

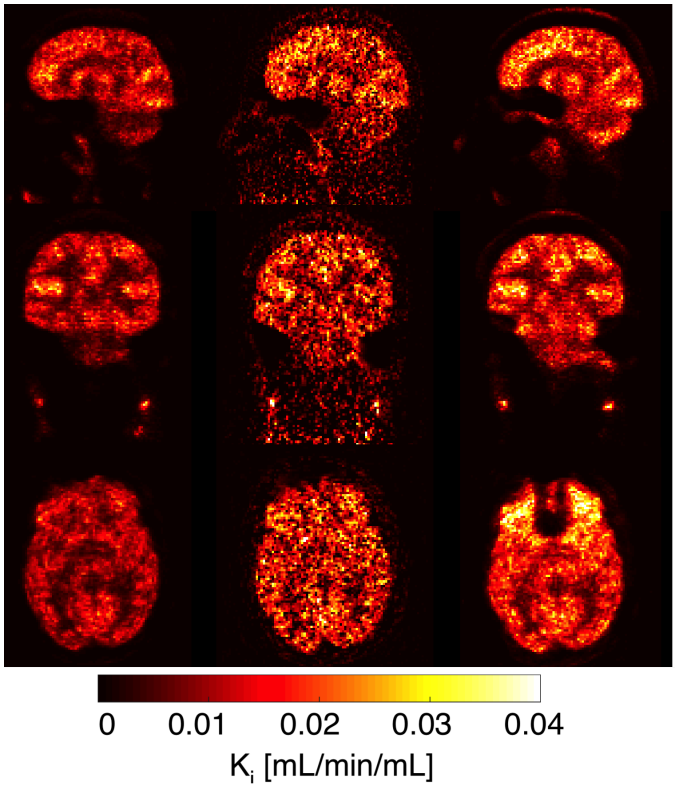

Fig. 6: Sagittal, coronal and axial views (top to bottom) of voxelised K_i values for MC direct, MC indirect and noMC direct (left to right).

motion occurs at 900 s in transformed Patlak time.

Using Fig. 4, the time period over which the Patlak analysis would be performed was established. The time frames that were then used for the analysis are shown in Fig. 5, both for the noMC and MC methods. Both methods contain 7 time frames, but in the case of noMC the time frames were evenly distributed, whereas in the case of MC they were altered to produce motionless frames. By comparing Fig. 5 with Fig. 3, it can be seen that the gaps in the MC time frames align with the detected motion.

In Fig. 6, the sagittal, coronal and axial views of voxelised K_i values can be seen for the three different methods. It can be seen that the MC direct method is particularly noisy, and it is difficult to distinguish different brain subregions. Furthermore, in the sagittal view of noMC direct (top right), it can be seen that the inferior frontal lobe is underestimated. From these images, it can therefore be concluded that, of the three methods, MC direct can produce images that are less noisy than MC indirect and with less artefacts than noMC direct.

The resulting K_i of the left temporal lobe for MC direct, MC indirect and noMC direct was 0.99, 1.16 and 1.21 $\times$ 10^{-2} mL/min/mL, with standard deviations of the voxels in the VOI of 54.0, 79.6 and 79.5 %, respectively. The reduced standard deviation in the case of MC direct implies greater precision compared to the other two methods. This is likely due to the decrease of noise compared to MC indirect, and reduction of artefacts compared to noMC direct.

IV. Conclusion

This paper demonstrates the implementation of direct Patlak reconstruction with MC in SIRF.

By studying a larger cohort of patients, further investigations will be carried out as to the improvements that the MC direct method can bring over conventional methods.

It should be noted that this method is equally applicable to non-rigid problems, such as gated dynamic reconstructions. This will be the focus of future work. Since motion in head scans is typically small, the advantages of MC are expected to be greater when applied to data acquired in other areas of the body.

Another focus of research in the near future is the implementation of anatomical parametric priors. Such priors will make greater use of the available MR data, furthering synergy between the two modalities.

Acknowledgement

We thank Francesco Fraioli (UCLH) for the clinical data. This work was supported by UK EPSRC under Grants EP/M022587/1 and EP/P022200/1.

References

[1] E. Ovtchinnikov *et al.*, *IEEE PSMR Conf. Proc.*, 2015.
[2] R. Brown *et al.* PSMR Conf., 2018.
[3] B. Fischl, *NeuroImage*, vol. 62, no. 2, pp. 774 – 781, 2012.
[4] A. Rashidnasab *et al.*, *IEEE PSMR Conf. Proc.*, pp. 3–4, 2017.
[5] P. J. Schleyer *et al.*, *Phys. Med. Biol*, vol. 60, no. 16, pp. 6441–6458, 2015.
[6] C. Tsoumpas *et al.*, *Med. Phys.*, vol. 35, no. 4, pp. 1299–1309, 2008.
[7] J. Matthews *et al.*, *Phys. Med. Biol*, vol. 42, no. 6, p. 1155, 1997.
[8] K. Thielemans *et al.*, *Phys. Med. Biol.*, vol. 57, no. 4, pp. 867–883, 2012.
[9] M. Modat *et al.*, *Journal Med. Im.*, vol. 1, no. 2, p. 024003, 2014.
[10] B. A. Thomas *et al.*, *Phys. Med. Biol.*, vol. 61, p. 7975, 2016.